ISSN 1070-3284, Russian Journal of Coordination Chemistry, 2009, Vol. 35, No. 12, pp. 891–895. © Pleiades Publishing, Ltd., 2009.

Organic-Inorganic Hybrid Supramolecular Architecture Constructed from Keggin-Type $[PMo_{12}O_{40}]^{3-}$ Clusters and Transition Metal Complexes[1]

J. W. Zhao, X. F. Zhang, P. T. Ma, Y. Q. Feng, J. P. Wang, and J. Y. Niu*

Institute of Molecular and Crystal Engineering, School of Chemistry and Chemical Engineering, Henan University, Kaifeng 475004, P.R. China

**e-mail: jyniu@henu.edu.cn*

Received February 24, 2009

Abstract—A Keggin organic-inorganic hybrid polyoxometalate combined with nickel complex $[Ni(Dmf)_3(H_2O)][HPMo_{12}O_{40}] \cdot (Dmf) \cdot 2H_2O$ (**I**) has been synthesized and structurally characterized by elemental analysis, IR spectrum, TG analysis, cyclic voltammetry, and single-crystal X-ray diffraction. Interestingly, a two-dimensional supramolecular network is constructed by the $[PMo_{12}O_{40}]^{3-}$ polyanions, $[Ni(Dmf)_3(H_2O)]^{2+}$ cations, and water molecules *via* hydrogen-bonding interactions. The cyclic voltammetric measurements illustrate that the $[PMo_{12}O_{40}]^{3-}$ polyanion is the electrochemical redox active center of **I** in the solution.

DOI: 10.1134/S1070328409120057

INTRODUCTION

The synthesis and exploitation of organic-inorganic hybrid compounds is still very active due to the possibility of combining the different characteristics of the components to obtain unusual structures, properties, and applications [1–4]. Meanwhile, polyoxometalates (**POM**) are used as remarkable useful inorganic building blocks owing to their molecular and electronic structural diversity and their significance in quite diverse disciplines ranging from catalysis, electrochemical and imaging to material science [5–9]. Thus, in recent years, a large number of hybrids built by POM associated with various transition metal complexes have been reported [10–14], in which the transition metal coordination complexes act as charge compensation cations and/or become a part of the inorganic POM frameworks. In the POM-based supramolecular architectures, basically, weaker intermolecular forces (including hydrogen bond interactions, π–π stacking interactions, van der Waals forces) are often utilized [15–17]. As we know, the most studied POM are the Keggin family, which can be represented by $[XM_{12}O_{40}]^{n-}$. As a continuous work, here we report a Keggin organic-inorganic hybrid polyoxometalate combined with nickel complexes $[Ni(Dmf)_3(H_2O)][HPMo_{12}O_{40}] \cdot (Dmf) \cdot 2H_2O$ (**I**), which are characterized by IR spectrum, cyclic voltammetry, TG analysis, and X-ray single-crystal diffraction.

[1] The article is published in the original.

EXPERIMENTAL

Materials and methods. The raw material of saturated Keggin-type precursor $H_3PMo_{12}O_{40} \cdot nH_2O$ was prepared according to the literature [18] and identified by IR spectra. Other reagents were obtained from commercial resources and used without further purification. Elemental analyses (C, H, and N) were performed on a Perkin Elmer 240C elemental analyzer. The IR spectrum was recorded from a sample powder pelletized with KBr on a Nicolet 170 SXFT-IR spectrometer over a range of 4000–400 cm^{-1}. The TG analysis was conducted on Perkin Elmer 7 analyzer in a nitrogen atmosphere with a heating rate of 10°C/min from 25 to 700°C. Cyclic voltammograms were obtained on an LK98BII electrochemical analyzer at room temperature. A glassy carbon (diameter 3 mm) electrode was employed as the working electrode. The electrode underwent ultrasonic washing for 3 min and was washed with water and enthanol prior to every measurement. A platinum rod (diameter 2 mm) was used as the counter electrode. The reference electrode was SCE. The scan rate was 100 V s^{-1}.

Synthesis of compound I. $H_3[PMo_{12}O_{40}] \cdot nH_2O$ (0.38 g) was dissolved in 20 ml of water and $NiCl_2 \cdot 6H_2O$ (0.28 g) was added with stirring. The resulting solution was filtered after 10 min, and then 2 ml DMF was added dropwise to the filtrate. The filtrate was kept at of room temperature for 3 weeks. Green crystals of **I**

Table 1. Crystallographic data and structure refinement summary for complexes **I**

Parameter	Value
Crystal system	Triclinic
Space group	$P\bar{1}$
a, Å	13.0307(13)
b, Å	13.4994(13)
c, Å	14.9265(15)
α, deg	95.4260(10)
β, deg	98.0060(10)
γ, deg	101.6670(10)
V, Å^3	2525.9(4)
Z	2
ρ_{calcd}, g cm^{-3}	2.930
μ, mm^{-1}	3.385
F(000)	2116
Crystal size, mm	0.19 × 0.14 × 0.11
Limiting indices	$-15 \le h \le 12$ $-16 \le k \le 16$ $-16 \le l \le 17$
Reflections collected/unique	12946/8809 (R_{int} = 0.0247)
Goodness-of-fit on F^2	1.002
Final R indices ($I > 2\sigma(I)$)	R_1 = 0.0276, wR_2 = 0.0736
R indices (all data)	R_1 = 0.0298, wR_2 = 0.0750
Largest difference peak and hole, e Å^{-3}	1.084 and –1.184

were isolated in a 30% yield (based on $H_3[PMo_{12}O_{40}] \cdot nH_2O$).

For $C_{12}H_{35}N_4O_{47}PNiMo_{12}$			
anal. calcd, %:	C, 6.47;	H, 1.58;	N, 2.51.
Found, %:	C, 6.45;	H, 1.61;	N, 2.49.

X-ray crystallography. A crystal of **I** (dimensions 0.19 × 0.14 × 0.11 mm) was carefully selected under an optical microscope and glued at the tip of a thin glass fiber with cyanoacrylate (superglue) adhesive. Intensity data were collected on a Bruker APEX-II CCD detector at 296(2) K with MoK_α radiation (λ = 0.71073 Å). The structures were solved by direct methods and refined by the full-matrix least-squares method on F^2 using the SHELXTL–97 package [19]. Intensity data were corrected for the Lorentz and polarization effects, as well as for empirical absorption. All of the non-hydrogen atoms were refined anisotropically. The crystallographic data are listed in Table 1. The atomic coordinates and other parameters of structure **I** have been deposited with the Cambridge Crystallographic Data Center (no. 714944; deposit@ccdc.cam.ac.uk).

RESULTS AND DISCUSSION

Single-crystal X-ray structural analysis indicates that the structural unit of **I** contains one Keggin $[PMo_{12}O_{40}]^{3-}$ polyanion, one $[Ni(Dmf)_3(H_2O)]^{2+}$ cation, one free Dmf molecule, one proton, and two lattice water molecules (Fig. 1). The polyanion $[PMo_{12}O_{40}]^{3-}$ exhibits a classical Keggin-type structure. The polyanion is built by a central PO_4 tertrahedron surrounded by twelve MoO_6 octahedra. Twelve MoO_6 octahedra are grouped into four trimetallic Mo_3O_{13} units in the edge-sharing mode, each of which is made up of three MoO_6 octahedra in the edge-sharing mode. The four trimetallic units Mo_3O_{13} are linked by sharing corners and combined with the central PO_4 tetrahedron. The central P atom exhibits the four-coordinate tetrahedral geometry. The bond distances and angles found in the polyoxoanion in **I** are very similar to those reported in the literature [20–22]. In the discrete $[Ni(Dmf)_3(H_2O)]^{2+}$ cation, the nickel atom is coordinated by four oxygen atoms from three Dmf ligands and one water ligand with the Ni–O distances of 1.930(3)–1.958(3) Å and ONiO angles of 88.64(12)°–178.70(14)° (*cis*-ONiO angles:

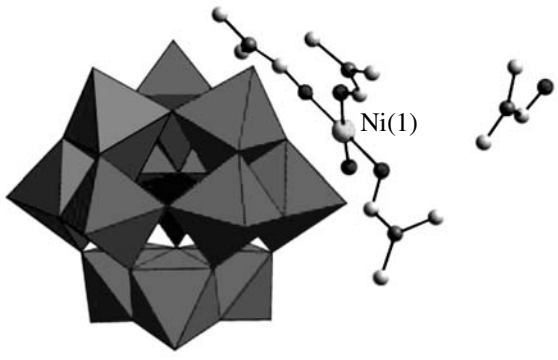

Fig. 1. The structural unit of **I** with partial atom labeling scheme. Gray octahedron is MoO_6, black tetrahedron is PO_4. The protons and lattice water molecules are omitted for clarity.

Table 2. Geometrical parameters of hydrogen bonding O–H···O interactions for **I***

D–H···A	Distance, Å		Angle DHA, deg	Coordinates of A atom
	H···A	D···A		
O(3*w*)–H(3*A*w)···O(31)	2.13	2.904(5)	154	$-x+1, -y+4, -z$
O(3*w*)–H(3*A*w)···O(2)	2.65	3.078(5)	113	$x+1, y-1, z$
O(3*w*)–H(3*Bw*)···O(23)	2.08	2.838(5)	151	$x, y-1, z$
O(1*w*)–H(1*Aw*)···O(2W)	1.85	2.673(5)	172	x, y, z
O(1*w*)–H(1*Bw*)···O(25)	2.01	2.820(4)	167	$-x, -y+5, -z$
O(2*w*)–H(2*Aw*)···O(33)	2.09	2.895(4)	163	$x, y-1, z$
O(2*w*)–H(2*Bw*)···O(1W)	2.49	3.121(5)	134	$-x, -y+4, -z$
O(2*w*)–H(2*Bw*)···O(1)	2.49	3.227(4)	149	$-x, -y+5, -z$

* O–H 0.83 Å.

88.64(12)°–91.04(13)°; *trans*-ONiO angles: 176.70(15)°–178.70(14)°). Bond valence sum calculations show that the oxidation state of the nickel atom is +2 [23].

It should be noted that **I** exhibits extensive hydrogen bonding interactions between the water ligands (O(1*w*)) on $[Ni(Dmf)_3]^{2+}$ cations, lattice water molecules (O(2*w*), O(3*w*)), and oxygen atoms (O(1), O(2), O(23), O(25), O(31), O(33)) from Keggin polyanion $[PMo_{12}O_{40}]^{3-}$ with the O(1*w*)···O(2*w*), O(1*w*)···O(25), O(2*w*)···O(1), O(2*w*)···O(33), O(3*w*)···O(2), O(3*w*)···O(23), and O(3*w*)···O(31) distances of 2.673, 2.820, 3.227, 2.895, 3.078, 2.838, and 2.904 Å, respectively (Table 2). Therefore, supramolecular interactions play a major role in the formation of the layer structure. The polyanions along the *xy* axis are linked together by O(3*w*) via the hydrogen-bonding interactions, forming supramolecular 1D chain structure (Fig. 2), and adjacent chains are further joined by O(1), O(2*w*) to construct a 2D network parallel to the *xy* plane (Fig. 3).

In the IR spectrum of **I**, four characteristic peaks of the Keggin-type polyoxoanion are observed at 1058, 962, 876, and 806 cm^{-1}, which are ascribed to the $\nu(P–O_a)$, $\nu(Mo–O_t)$, $\nu(Mo–O_b–Mo)$, and $\nu(Mo–O_c–Mo)$ stretching vibrations. In comparison with the IR spectrum of the precursor $H_3PMo_{12}O_{40} \cdot nH_2O$, the characteristic peaks of **I** have different shifts. This phenomenon indicates that there are strong interactions between the polyanions and metal coordination cations in addition to the effect of the protonation state of the polyanion in part being eliminated (the starting material $H_3PMo_{12}O_{40} \cdot nH_2O$ is indeed fully protonated) in the solid state. The vibration peak of C=O in the Dmf ligands in **I** has a red shift from 1678 to 1645 cm^{-1}. This result shows that electron atmosphere vibration frequency over the carbonyl group is decreased, which further confirms that the Dmf molecules as ligands have been coordinated to Ni^{2+} ions by their oxygen atoms.

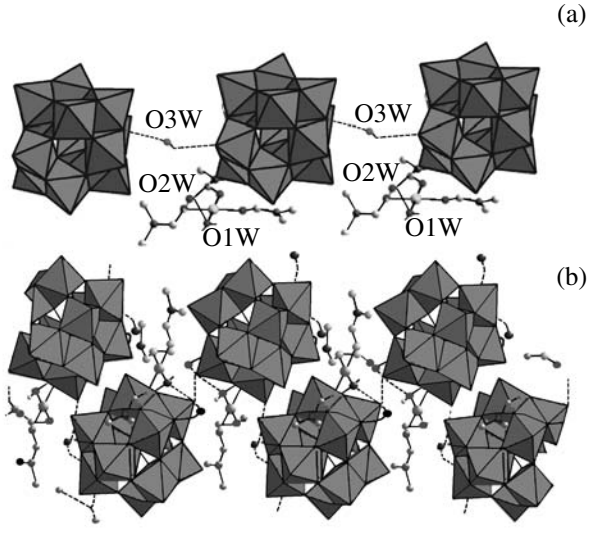

Fig. 2. View of the one-dimensional chain-like alignment along the *x* (a) and the *y* axis (b).

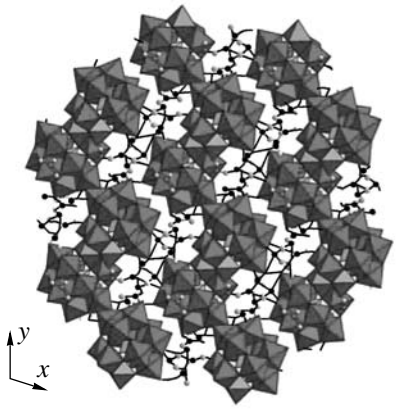

Fig. 3. Perspective drawing of the two-dimensional infinite network in **I**.

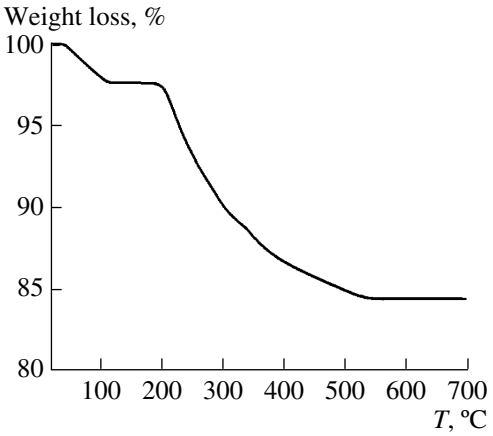

Fig. 4. The TG curve of **I**.

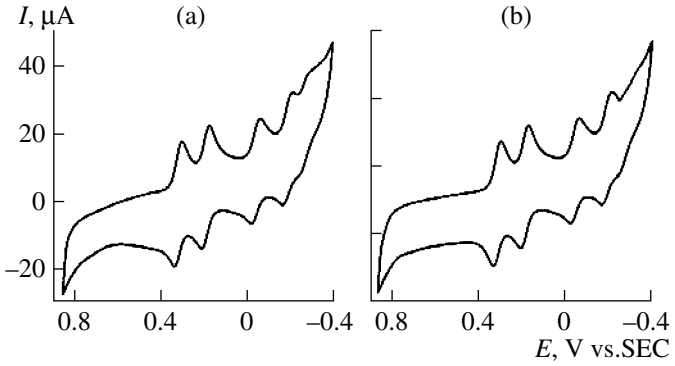

Fig. 5. Cyclic voltammograms of $H_3[PMo_{12}O_{40}] \cdot nH_2O$ (a) and **I** (b) in the pH 1.5 medium.

The TG curve of **I** shows two stage weight loss giving a total loss of 15.53% of its initial weight in a range of 27–530°C (Fig. 4). The first weight loss is 2.46% in a temperature range of 27–206°C corresponding to the release of two lattice water molecules and one free Dmf molecule (calcd. 2.42%). The second weight loss of 13.07%) from 206 to 530°C attributed to the removal of one coordinated water, and three Dmf molecules and the dehydration of one proton (calcd. 13.10%).

Table 3. Cathodic (E_{cp}), anodic (E_{ap}), and half-wave potential ($E_{1/2}$)

E_{cp}, V	E_{ap}, V	ΔE_p, mV	$E_{1/2}$, V
	I		
0.302	0.337	35	0.319
0.177	0.209	32	0.193
–0.057	–0.021	36	–0.039
–0.206	–0.169	37	–0.188
	$H_3[PMo_{12}O_{40}] \cdot nH_2O$		
0.306	0.340	34	0.323
0.179	0.212	33	0.196
–0.057	–0.022	35	–0.040
–0.201	–0.170	31	–0.186

Electrochemical measurements for $H_3[PMo_{12}O_{40}] \cdot nH_2O$ and **I** were performed to investigate their redox properties in secondary distilled water containing 0.5 mol/l H_2SO_4 as the supporting electrolyte (Fig. 5). Table 3 summarizes the cathodic ($\boldsymbol{E_{cp}}$) and anodic potentials ($\boldsymbol{E_{ap}}$) and the half-wave potentials ($\boldsymbol{E_{1/2}}$). In comparison with the cyclic voltammogram of $H_3[PMo_{12}O_{40}] \cdot nH_2O$ (Fig. 5a), the $[PMosO_{40}]^{3-}$ polyanion in **I** exhibits a kinetically stable and reproducible cyclic voltammetric pattern. The CV voltammograms of **I** and $H_3[PMo_{12}O_{40}] \cdot nH_2O$ show four well-defined redox waves, indicating that both **I** and $H_3[PMo_{12}O_{40}] \cdot nH_2O$ undergo four two-electron charge-transfer processes. The CV voltammogram comparison of **I** and $H_3[PMo_{12}O_{40}] \cdot nH_2O$ illustrates that the $[PMo_{12}O_{40}]^{3-}$ polyanion is the electrochemical redox active center of **I** in the solution.

ACKNOWLEDGMENTS

This work was supported by the National Natural Science Foundation of China, Program for New Century Excellent Talents at the University of Henan Province, the Specialized Research Fund for the Doctoral Program of University Prominent Research Talents and the Natural Science Foundation of Henan Province.

REFERENCES

1. Niu, J.Y., Han, Q.X., and Wang, J.P., *J. Coord. Chem.*, 2003, vol. 56, p. 523.
2. Wang, J.P., Wu, Q., and Niu, J.Y., *Chin. J. Inorg. Chem.*, 2002, vol. 18, p. 957.
3. Hussain, F., Kortz, U., Keita, B., et al., *Inorg. Chem.*, 2006, vol. 45, p. 761.
4. Shen, Y., Liu, J., Jiang, J., et al., *J. Phys. Chem., B*, 2003, vol. 107, p. 9744.
5. Pope, M.T., *Heteropoly and Isopoly Oxometalates,* Berlin: Springer, 1983, p. 1.
6. Pope, M.T. and Muler, A., *Angew. Chem. Int. Ed.*, 1991, vol. 30, p. 34.
7. *Polyoxometalates: From Platonic Solids To Anti-Retroviral Activity*, Pope, M.T. and Muller, A., Eds., Dordrecht (The Netherlands): Kluwer Academic, 1994.
8. Pope, M.T., *Comprehensive Coordination Chemistry II: From Biology to Nanotechnology*, Wedd, A.G., Ed., Oxford (U.K.): Elsevier, 2004, vol. 4, p. 635.
9. Hill, C.L., *Comprehensive Coordination Chemistry II: From Biology to Nanotechnology*, Wedd, A.G., Ed., Oxford: Elsevier, 2004, vol. 4, p. 679.
10. Niu, J.Y., Wang, Z.L., and Wang, J.P., *J. Coord. Chem.*, 2004, vol. 57, p. 411.
11. Niu, J.Y., Wang, Z.L., and Wang, J.P., *Polyhedron*, 2004, vol. 23, p. 773.
12. Wang, X.L., Lin, H.Y., Qi, Y.F., et al., *J. Solid State Chem.*, 2008, vol. 181, p. 556.
13. Sha, J.Q., Wang, C., Peng, J., et al., *Inorg. Chem. Commun.,* 2007, vol. 10, p. 1321.
14. Zhang, Z.M., Yao, S., Wang, E.B., et al., *J. Solid State Chem.*, 2008, vol. 181, p. 715.
15. Zhang, H., Duan, L., Lan, Y., et al., *Inorg. Chem.*, 2003, vol. 42, p. 8053.
16. Zheng, P.Q., Ren, Y.P., Long, L.S., et al., *Inorg. Chem.*, 2005, vol. 44, p. 1190.
17. Zhu, Y., Xiao, Z.C., Ge, N., et al., *Cryst. Growth Des.*, 2006, vol. 6, p. 1620.
18. Claude, R.D., Raymonde, F., and Rene, T., *Inorg. Chem.*, 1983, vol. 22, p. 207.
19. Sheldrick, G.M., *SHEXTL-97, Programs for Crystal Structure Refinement*, Göttingen (Germany), Univ. of Göttingen, 1997.
20. Niu, J.Y., Wang, J.P., and Bo, Y., *J. Chem. Crystallogr.*, 2000, vol. 30, p. 43.
21. Williamson, M.M., Bouchard, D.A., and Hill, C.L., *Inorg. Chem.*, 1987, vol. 26, p. 1436.
22. Neier, A., Trojanowski, C., and Mattes, R., *J. Chem. Soc., Dalton, Trans.*, 1996, p. 2521.
23. Brese, N.E. and O'Keeffe, M., *Acta Crystallogr., Sect. B: Struct. Sci.*, 1991, vol. 47, p. 192.